Cell

Structure of the Rb C-Terminal Domain Bound to E2F1-DP1: A Mechanism for Phosphorylation-Induced E2F Release

Seth M. Rubin,[1] Anne-Laure Gall,[1,2] Ning Zheng,[1,3] and Nikola P. Pavletich[1,*]
[1] Structural Biology Program and Howard Hughes Medical Institute, Memorial Sloan-Kettering Cancer Center, New York, NY 10021, USA
[2] Present Address: Laboratoire de Neurobiologie, Ecole Normale Supérieure, Paris, France.
[3] Present Address: Department of Pharmacology, University of Washington, Seattle, WA 98195, USA.
*Contact: nikola@xray2.mskcc.org
DOI 10.1016/j.cell.2005.09.044

SUMMARY

The retinoblastoma (Rb) protein negatively regulates the G1-S transition by binding to the E2F transcription factors, until cyclin-dependent kinases phosphorylate Rb, causing E2F release. The Rb pocket domain is necessary for E2F binding, but the Rb C-terminal domain (RbC) is also required for growth suppression. Here we demonstrate a high-affinity interaction between RbC and E2F-DP heterodimers shared by all Rb and E2F family members. The crystal structure of an RbC-E2F1-DP1 complex reveals an intertwined heterodimer in which the marked box domains of both E2F1 and DP1 contact RbC. We also demonstrate that phosphorylation of RbC at serines 788 and 795 destabilizes one set of RbC-E2F-DP interactions directly, while phosphorylation at threonines 821 and 826 induces an intramolecular interaction between RbC and the Rb pocket that destabilizes the remaining interactions indirectly. Our findings explain the requirement of RbC for high-affinity E2F binding and growth suppression and establish a mechanism for the regulation of Rb-E2F association by phosphorylation.

INTRODUCTION

The transition from the G1 to the S phases of the cell cycle marks an irreversible commitment to DNA synthesis and proliferation and is strictly regulated by positive and negative growth-regulatory signals. The G1-S transition is controlled by the Rb-E2F pathway, which links growth-regulatory pathways to a transcription program required for DNA synthesis, cell cycle progression, and cell division (Dyson, 1998; Weinberg, 1995). This transcription program is activated by the E2F transcription factors and repressed by E2F-Rb complexes. E2F overexpression or Rb inactivation is sufficient to induce S phase entry, whereas Rb overexpression can arrest cycling cells in G1, demonstrating that the Rb-E2F pathway is central to the control of the G1-S transition (Dyson, 1998; Weinberg, 1995).

In quiescent cells or cells in early G1, the Rb protein binds to the E2F transcription factors and blocks their transactivation domain. Rb also recruits transcriptional co-repressors such as histone deacetylases (HDAC) and chromatin-remodeling complexes, resulting in the repression of E2F-responsive promoters (Dyson, 1998). Mitogenic growth factors lead to the sequential activation of the cyclin-dependent kinase (Cdk)-Cyclin complexes Cdk4/6-CyclinD and Cdk2-CyclinE, which hyperphosphorylate Rb and thereby cause the release of active E2F (Dyson, 1998; Weinberg, 1995). The Rb pathway thus ensures that S phase entry strictly depends on growth-factor signals.

The importance of Rb in the control of cell proliferation is underscored by the deregulation of this pathway in a majority of cancer cases, which occurs either by mutation or deletion of Rb, or by alterations in the upstream Cdk, Cyclin, and Cdk-inhibitory proteins (Sherr, 1996; Weinberg, 1995). Rb is also inactivated by DNA tumor viruses such as the human papillomavirus (HPV), adenovirus, and the simian virus 40 (SV40), all of which express proteins that induce S phase by binding to Rb and releasing active E2Fs (Nevins, 1994).

In humans, there are at least six closely related E2F proteins (E2F1 through E2F6) and two Rb homologs (p107 and p130), which are commonly referred to as pocket proteins. The E2F proteins have similar core DNA-sequence specificity, but they differ in their ability to drive quiescent cells into the cell cycle and in their relative promoter distribution in G1 and S (Trimarchi and Lees, 2002). E2F1 through E2F3 are typically associated with active promoters in S phase, while E2F4 through E2F6 with repressed promoters in G0 or early G1. These differences are correlated with the preferences of E2Fs for different Rb family members

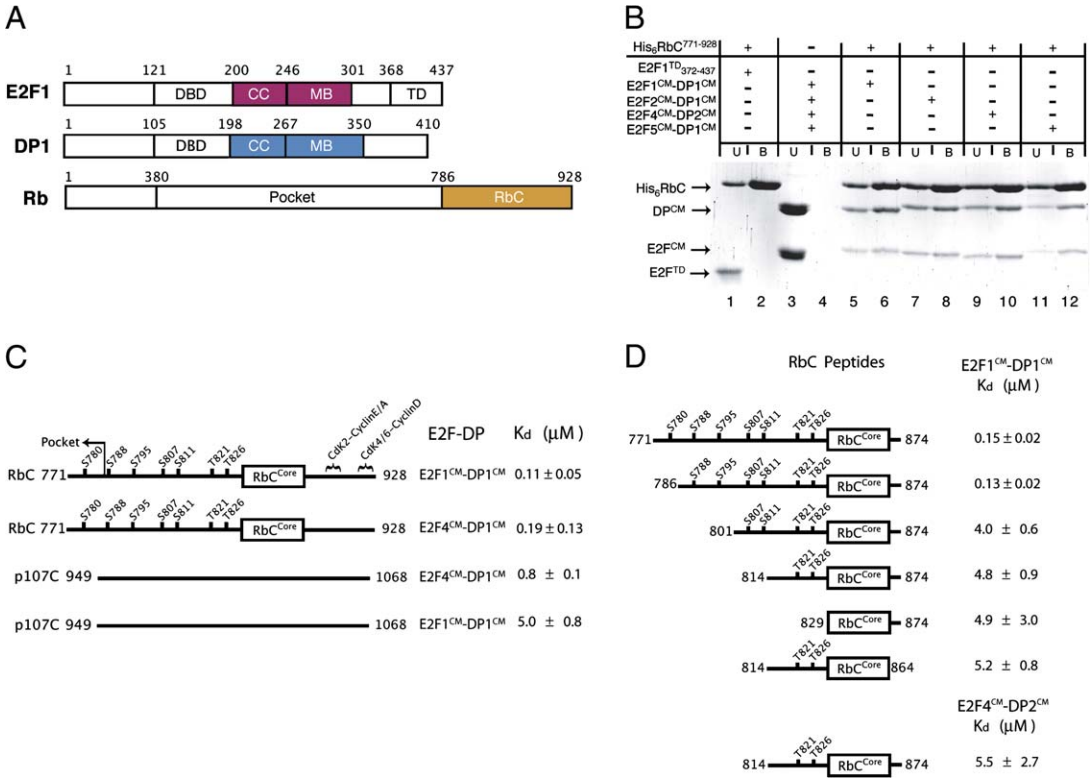

Figure 1. The C-Terminal Domains of the Rb and p107 Pocket Proteins Contain a General E2F^{CM}-DP^{CM} Binding Site

(A) Schematic representation of the previously described domains of E2F1, DP1, and Rb. The boundaries of the CC and MB domains are according to results presented here.

(B) RbC binding is a general property of both E2F subfamilies, and both DP1 and DP2, which are closely related, support RbC-E2F^{CM}-DP^{CM} binding. Ten micromolar purified His$_6$RbC$^{771–928}$ was incubated with 10 μM of the indicated purified E2F^{CM}-DP^{CM} heterodimer or with the E2F transactivation domain used as a negative control. Reactions were precipitated with Ni^{2+}-NTA resin, and the unbound (U) and eluted bound (B) fractions were analyzed with SDS-PAGE and Coomassie staining.

(C) E2F^{CM}-DP^{CM} binding is common to Rb and p107. The dissociation constants (K_d) for the binding of RbC or p107 to E2F1^{CM}-DP1^{CM} and E2F4^{CM}-DP1^{CM} complexes were determined by isothermal titration calorimetry (ITC) and calculated as the average and standard deviation from two to four independent measurements (titration data are shown in Supplemental Data, Section 1). The RbC^{core}-E2F^{CM}-DP^{CM} interacting motif defined in this study is shown by a box. For Rb, the locations of the Ser/Thr residues shown to be phosphorylated by Cdk-Cyclin complexes and of the reported docking sites for these kinases are also indicated. The Rb C-terminal fragment used includes 15 residues from the end of the pocket structure, which is indicated by an arrow.

(D) RbC^{core} binds E2F^{CM}-DP^{CM} through a bipartite interaction. The dissociation constants for the binding of truncated RbC fragments to E2F1^{CM}-DP1^{CM} or to E2F4^{CM}-DP2^{CM} were determined by ITC as in (C).

(Trimarchi and Lees, 2002). E2F1, E2F2, and E2F3 are found associated with Rb, and E2F5 with p130. E2F4, which is the most abundant family member, is found associated primarily with p107 and to a lesser extent with Rb and p130. E2F proteins form heterodimers with one of two DP proteins, which are distantly related to the E2F proteins. Heterodimerization has been shown to enhance the Rb binding, DNA binding, and transactivation activities of E2Fs (Bandara et al., 1994; Helin et al., 1993b; Krek et al., 1993).

The six E2F and two DP family members all contain a DNA binding domain (DBD), predicted coiled-coil (CC) domain, and marked-box (MB) domain (Figure 1A). The transactivation domain (TD) is present only in E2F1 through E2F5. Rb contains a 379 residue N-terminal domain of unknown function, a 406 residue middle domain commonly referred to as the pocket, and a 143 residue C-terminal domain (RbC; Figure 1A). The pocket domain, which is best conserved among Rb paralogs, directly binds to and blocks the E2F transactivation domain (Flemington et al., 1993; Helin et al., 1993a). The pocket of Rb is necessary but not sufficient for growth suppression, which additionally requires RbC (Qin et al., 1992). RbC is also required for high-affinity binding to E2F-DP complexes and for maximal repression of E2F-responsive promoters (Hiebert, 1993; Hiebert et al., 1992; Qin et al., 1992). The importance of the RbC domain is recapitulated in the Rb paralogs p107 and p130, which have conserved sequences C-terminal to their pocket domains that are required for growth suppression, high-affinity binding to their preferred E2F-DP complexes, and maximal repression of E2F-responsive promoters (Zhu et al., 1995). These observations suggest a role for the C-terminal domains of Rb and its paralogs in E2F-DP binding.

A general RbC-E2F-DP interaction has also been suggested by studies of the HPV E7, adenovirus E1A, and

SV40 large tumor antigen proteins that cause the release of E2F. These proteins share a common LxCxE sequence motif that binds to the Rb pocket domain with high affinity but does not cause the release of E2F (Patrick et al., 1994; Raychaudhuri et al., 1991; Zalvide et al., 1998). E2F release requires additional viral-protein domains, which in the case of HPV E7 has been shown to bind RbC (Patrick et al., 1994). In addition, the adenovirus E4-6/7 protein, which blocks the association of E2F with Rb, has been shown to bind to the E2F MB domain (Jost et al., 1996; O'Connor and Hearing, 1994). Taken together, these findings raised the possibility that RbC binds to the E2F MB domain and that interference with this association contributes to the release of E2F by viral proteins. A recent study showed that an Rb C-terminal fragment can bind to a truncated E2F1 protein that lacks the transactivation domain (Dick and Dyson, 2003). However, this interaction was shown to be E2F1 specific and was implicated in an apoptotic function unique to E2F1.

The mechanism through which E2F is dissociated by Rb hyperphosphorylation has not been well understood, but most studies point to a hierarchical series of Rb phosphorylation events cumulatively affecting the stability of the Rb-E2F complex (Brown et al., 1999; Chellappan et al., 1991; Harbour et al., 1999; Knudsen and Wang, 1997; Lundberg and Weinberg, 1998). Six of the sixteen consensus Cdk phosphorylation sites of Rb map to the RbC, raising the possibility that if a general RbC-E2F interaction does exist, it may be involved in the phosphorylation-induced release of E2F.

Here, we demonstrate an interaction between RbC and the CC-MB domains of E2F-DP heterodimers and present the crystal structure of an RbC-E2F1-DP1 complex. The structure in conjunction with biochemical and biophysical data indicate that the RbC-E2F-DP interaction (1) is shared by all E2F and Rb family members, (2) contributes to the preference of p107/p130 for the E2F4 subfamily, and (3) is negatively regulated by RbC hyperphosphorylation.

RESULTS

An RbC-E2F-DP Interaction Common to Rb and E2F-DP Family Members

To investigate the possibility of a general interaction between the C-terminal domains of the pocket proteins and the MB domains of their respective E2F-DP partners, we first used limited proteolysis to better define the structural organization of the E2F-DP heterodimer. Extending previous work showing that the E2F-DP DNA binding domains are connected to the CC-domains through an ~five residue flexible linker (Zheng et al., 1999), we found that the E2F2-DP1 heterodimer has a protease-resistant structural domain consisting of residues 209–304 of E2F2 and 199–350 of DP1 (data not shown). These fragments include the CC and MB domains, shown to be required for E2F-DP heterodimerization (Helin et al., 1993b) and notably lack the E2F transactivation domain (Figure 1A).

We assessed whether this E2F2-DP1 heterodimer (hereafter E2F2^{CM}-DP1^{CM}) or the corresponding E2F1^{CM}-DP1^{CM}, E2F4^{CM}-DP2 ^{CM}, and E2F5^{CM}-DP1^{CM} heterodimers bind RbC using a Ni^{2+}-His_6 affinity-precipitation assay. For this experiment, we used an Rb fragment (residues 771–928; hereafter RbC$^{771–928}$) that contains RbC and the preceding 15 residue region from the end of the pocket domain. We incubated 10 μM purified His_6RbC$^{771–928}$ with 10 μM of each purified E2F^{CM}-DP^{CM} heterodimer, precipitated it using Ni^{2+}-NTA resin, eluted it with imidazole, and analyzed His_6RbC$^{771–928}$ bound proteins with SDS-PAGE and Coomassie staining. Figure 1B shows that RbC$^{771–928}$ bound all four E2F^{CM}-DP^{CM} heterodimers but did not bind the E2F1 transactivation domain used as a negative control.

We next measured the affinity of the RbC-E2F^{CM}-DP^{CM} interaction using isothermal titration calorimetry (ITC; see data in the Supplemental Data, Section 1, available with this article online). We found that RbC$^{771–928}$ binds to the E2F1^{CM}-DP1^{CM} complex with a dissociation constant (K_d) of 110 ± 50 nM (standard deviation from four independent measurements) and to the E2F4^{CM}-DP1^{CM} complex with a K_d of 190 ± 130 nM (SD from two experiments; Figure 1C). These K_d values are comparable to the Rb pocket domain-E2F1 transactivation domain K_d, which has been reported to be 340 nM and 400 nM in two independent ITC studies (Lee et al., 1998; Xiao et al., 2003). Our ITC data thus indicate that the RbC-E2F^{CM}-DP^{CM} interaction could be as important as the pocket-transactivation domain interaction for the formation of the Rb-E2F-DP complex. We suggest this observation provides an adequate explanation for the significant body of literature showing that RbC is required for high-affinity E2F-DP binding, for full repression of E2F-responsive promoters, and ultimately for growth suppression (Hiebert, 1993; Hiebert et al., 1992; Qin et al., 1992). In addition, the dissociation constants for the binding of RbC to the E2F1^{CM}-DP1^{CM} and the E2F4^{CM}-DP1^{CM} complexes are comparable within experimental error. Taken together with the Ni^{2+} precipitation data, these findings indicate that the ability to bind RbC is shared by the E2F1 and E2F4 subfamilies and both DP1 and DP2.

We next investigated whether p107 has a similar E2F^{CM}-DP^{CM} binding activity. The C-terminal domain of p107 and its close homolog p130 share only limited sequence homology with RbC, but like RbC, the p107 C terminus is required for growth suppression and high-affinity E2F binding (Zhu et al., 1995). Using ITC, we tested the binding of a p107 fragment encompassing the entire sequence following the pocket domain (residues 949–1068; hereafter p107C) to E2F-DP complexes. Figure 1C shows that p107C binds to the E2F4^{CM}-DP1^{CM} complex tightly with a K_d of 0.8 ± 0.1 μM and to the E2F1^{CM}-DP1^{CM} complex weakly with a K_d of 5.0 ± 0.8 μM. Taken together, our data indicate that E2F^{CM}-DP^{CM} binding is an activity common to the C-terminal domains of both Rb and p107 and that this activity contributes to the preference of p107 for E2F4 (Trimarchi and Lees, 2002).

RbC Binds to E2F^{CM}-DP^{CM} through a Bipartite Interaction

Limited proteolysis of an Rb protein containing the pocket and RbC domains suggested that RbC does not contain stable structural domains (data not shown), and NMR data indicate that the isolated RbC is unstructured in solution

(Supplemental Data, Section 2). We thus made successive N- and C-terminal truncations guided by sequence conservation to map the RbC region(s) involved in $E2F^{CM}$-DP^{CM} binding. The affinities of these Rb fragments for $E2F1^{CM}$-$DP1^{CM}$ were determined using ITC, and the results are listed in Figure 1D.

Deletion of the C-terminal 54 residues (875–928), shown to contain docking sites for the Cdk2-CyclinA/E and Cdk4/6-CyclinD binding complexes (Adams et al., 1999; Pan et al., 2001; Wallace and Ball, 2004), had no effect on the affinity for $E2F1^{CM}$-$DP1^{CM}$ ($RbC^{771–874}$ $K_d = 0.15 \pm 0.02$ μM), indicating that these residues are not involved in $E2F1^{CM}$-DP^{CM} binding. Deletion of the N-terminal 15 residues (771–785) that are part of the Rb pocket crystal structure (Lee et al., 1998) also had no effect on the affinity ($RbC^{786–874}$ $K_d = 0.13 \pm 0.02$ μM).

Deletion of the next 15 N-terminal residues of RbC (786-800) decreased the affinity by a factor of ~36 ($RbC^{801–874}$ $K_d = 4 \pm 1$ μM), indicating that residues 786–800 are involved in $E2F1^{CM}$-$DP1^{CM}$ binding. Further N-terminal deletions until residue 829 had no additional effect on the affinity ($RbC^{814–874}$ $K_d = 4.8 \pm 0.9$ μM and $RbC^{829–874}$ $K_d = 4.9 \pm 3$ μM). In light of the crystal structure described below, we made one additional C-terminal deletion of residues 865–874 and found that they are uninvolved in binding ($RbC^{814–864}$ $K_d = 5.2 \pm 0.8$ μM). Taken together, these data indicated that RbC contains two discontinuous regions that interact with $E2F1^{CM}$-$DP1^{CM}$. A core region between residues 829–864 (hereafter RbC^{core}) binds with a K_d of ~5 μM, while a secondary region within residues 786–800 (hereafter RbC^{nter}) contributes a 36-fold increase in affinity. This bipartite mode of RbC-E2F1-DP1 binding is mirrored in the binding of RbC to E2F4-DP1/2. As shown in Figure 1D, deletion of RbC^{nter} reduces the affinity of RbC for $E2F4^{CM}$-$DP2^{CM}$ 25-fold ($RbC^{814–874}$ $K_d = 5.0 \pm 0.8$ μM compared to 0.19 μM for $RbC^{771–874}$).

Building on these findings, we obtained crystals of a ternary complex consisting of $RbC^{829–874}$, which contains RbC^{core} but lacks RbC^{nter}, bound to the $E2F1^{CM}$-$DP1^{CM}$ heterodimer. The structure was determined by the multiwavelength anomalous diffraction (MAD) method using data from a selenomethionine-substituted complex and was refined at 2.55 Å resolution (Table 1). The refined model contains residues 829–872 of Rb, residues 201–301 of E2F1, and residues 199–346 of DP1.

Overall Structure of the $E2F1^{CM}$-$DP1^{CM}$-RbC^{core} Complex

The $E2F1^{CM}$-$DP1^{CM}$ heterodimer has an intertwined structure consisting of an intermolecular coiled coil, an intermolecular β sandwich, and several additional structural elements (Figure 2A). The coiled coil is formed by a 35 residue helix (eH1) from the E2F1 CC domain and a 48 residue helix (dH1) from the DP1 CC domain. The N-terminal half of the coiled coil has a canonical arrangement of helices (Lupas, 1996), but the remainder has larger helix-helix distances associated with contacts to other parts of the complex.

The intermolecular β sandwich structure is similar to the immunoglobulin fold (Bork et al., 1994). It consists of two four-stranded β sheets that pack across a mixed hydrophobic core involving both E2F1 and DP1 side chains (Figure 2A). Each sheet has a pair of strands from E2F1 and a pair of strands from DP1 (eS2, eS5, dS2, dS5 on one sheet and eS3, eS4, dS3, dS4 on the other; Figures 2A and 2B).

In addition to the intermolecular coiled coil and β sandwich, $E2F1^{CM}$-$DP1^{CM}$ contains five additional α helices (eH2, eH3, and dH2 to dH4) and a short two-stranded β sheet (eS1 and dS1; Figures 2A and 3A). These occur at nonanalogous positions in the E2F1 and DP1 primary sequences and in the tertiary structure (Figures 2A and 2B). Although both the coiled coil and β sandwich have 2-fold pseudosymmetry, the structure of the overall complex is asymmetric due to the location of the coiled coil at one end of the β sandwich and the nonanalogous E2F1 and DP1 helices.

The RbC fragment adopts a 32 residue strand-loop-helix structure followed by a 20 residue tail segment that lacks regular secondary structure (Figures 2A and 2B). The strand-loop-helix motif (rS1 and rH1) binds to one side of the β sandwich and interacts with both E2F1 and DP1. The rS1 strand extends one of the E2F1-DP1 β sheets by forming a fifth β strand alongside of eS3, while the rH1 helix packs against the partially exposed hydrophobic core of the β sandwich. Following the rH1 helix, the RbC tail loops around one end of the β sandwich, making additional contacts with E2F1 and DP1.

$E2F1^{CM}$-$DP1^{CM}$ Interactions and Preference for Heterodimerization

The E2F1-DP1 heterodimer interface buries ~6300 $Å^2$ of surface area compared to the hypothetical isolated monomers of the same structure. Intermolecular interactions are distributed throughout the E2F1 and DP1 polypeptides and involve the coiled coil, the β sandwich, and essentially all of the additional secondary-structure elements (Figures 2A and 2B). These additional structural elements also help anchor the coiled coil to the β sandwich (Figure 3A). The E2F1 and DP1 residues that make intermolecular contacts are either identical or conservatively substituted in their respective families (Figure 2B), consistent with observations that both DP1 and DP2 can heterodimerize with the first six E2F paralogs (Trimarchi and Lees, 2002).

The E2F1-DP1 interactions revealed by the crystal structure have several implications for understanding the preference of E2F proteins to form heterodimers with DP proteins and also help address the question of whether E2F proteins can form functional homodimers (Bandara et al., 1993; Helin et al., 1993b; Huber et al., 1993; Krek et al., 1993). We note that unlike the intermolecular coiled coil and β sandwich that are related by a 2-fold pseudosymmetry, many interactions involve nonanalogous structural elements of E2F and DP. For example, the E2F-specific eH2 helix interacts with dH1, and the E2F-specific eH3 helix interacts with dS4 and with the DP-specific dH2 (Figure 3A). These observations suggest that if E2F could form a homodimer, its structure would be significantly different from that of E2F1-DP1.

Even within the coiled coil, the intermolecular interactions often involve noninterchangeable hydrophobic and charged

Table 1. Statistics from the Crystallographic Analysis

Data Set	Native	Se λ1	Se λ2	Se λ3
Beamline	ID24 (APS)	X4A (NSLS)	X4A (NSLS)	X4A (NSLS)
Wavelength (Å)	0.94980	0.97916	0.97241	0.97929
Resolution (Å)	2.55	2.7	2.7	2.7
Observations	71,304	188,703	191,178	138,084
Unique reflections	19,350	35,326	35,584	36,140
Data coverage (%)	97.8	99.3	99.5	98.5
R_{sym} (%) (last shell: 2.55–2.64, 2.70–2.79)	5.3 (42.5)	6.1 (27.4)	6.1 (32.6)	5.6 (40.2)
MAD Analysis				
Resolution		20–3.0	20–3.0	20–3.0
Phasing power		1.09	1.62	—
R_{cullis}		0.83	0.69	—
Anomalous R_{cullis}		0.52	0.57	0.64
Mean FOM		0.68		
Refinement Statistics				
Resolution range (Å)	15.0–2.55			
Reflections ($\|F\|>0\sigma$)	17,600			
Total atoms	2459			
Number of water molecules	131			
R factor (%) (last shell: 2.55–2.62)	22.1 (27.3)			
R_{free} (%) (last shell: 2.55–2.62)	26.2 (28.4)			
Rmsd				
Bonds (Å)	0.009			
Angles (°)	1.157			
B factor (Å^2)	Main chain bond	1.47	Side chain bond	2.58

$R_{sym} = \Sigma_h\Sigma_i\ |I_{h,I} - I_h|/\Sigma_h\Sigma_i\ I_{h,i}$ for the intensity (I) of i observations of reflection h. Phasing power = $<F_{\lambda i}>/E$, where $<F_{\lambda i}>$ is the rms heavy atom structure factor and E is the residual lack of closure error. R_{cullis} is the mean residual lack of closure error divided by the dispersive or anomalous difference. R factor = $\Sigma||F_{obs}| - |F_{calc}||/\Sigma|F_{obs}|$, where F_{obs} and F_{calc} are the observed and calculated structure factors, respectively. R_{free} = R factor calculated using 5% of the reflection data chosen randomly and omitted from the start of refinement. Rmsd., root-mean-square deviations from ideal geometry and variations in the B factor of bonded atoms.

residues of E2F1 and DP1 (Supplemental Data, Section 3). For example, the acidic and basic residues that form intermolecular salt bridges are segregated to E2F1 and DP1, respectively. Such salt bridges play an important role in the preference of coiled coils to heterodimerize rather than homodimerize (Lupas, 1996). These observations suggest that if E2F could form a homodimeric coiled coil, its stability would be significantly lower than that of the E2F1-DP1 heterodimer.

To test this hypothesis, we assessed the binding of His_6-tagged $E2F1^{CM}$ to either $E2F1^{CM}$ or $DP1^{CM}$ using the Ni^{2+} affinity precipitation assay as described for Figure 1B. We incubated 10 μM His_6E2F1^{CM} with 10 μM of either the corresponding untagged $E2F1^{CM}$-$DP1^{CM}$ complex or untagged $E2F1^{CM}$ for 24 hr to allow for partial exchange. Figure 3B shows that His_6E2F1^{CM} bound approximately one-third of the total $DP1^{CM}$ in the reaction containing $E2F1^{CM}$-$DP1^{CM}$ but did not bind a detectable amount of $E2F1^{CM}$ (Figure 3B, lane 6). These data indicate a strong preference to form heterodimers over homodimers. When we incubated His_6E2F1^{CM} with untagged $E2F1^{CM}$ only, we could not detect any $E2F1^{CM}$ (Figure 3B, lane 8). We obtained similar results when the proteins were corefolded from urea (data not shown). In addition, NMR data suggest that $E2F1^{CM}$ is unstructured in the absence of DP1 (Supplemental Data, Section 2). These results confirm the structure-based prediction that the $E2F1^{CM}$ homodimer is less stable than the $E2F1^{CM}$-$DP1^{CM}$ heterodimer, and they provide an explanation for the observation that the DNA binding and transactivation activities of E2F1 are reduced in the absence of a DP partner (Bandara et al., 1993; Helin et al., 1993b; Huber et al., 1993; Krek et al., 1993; Zheng et al., 1999).

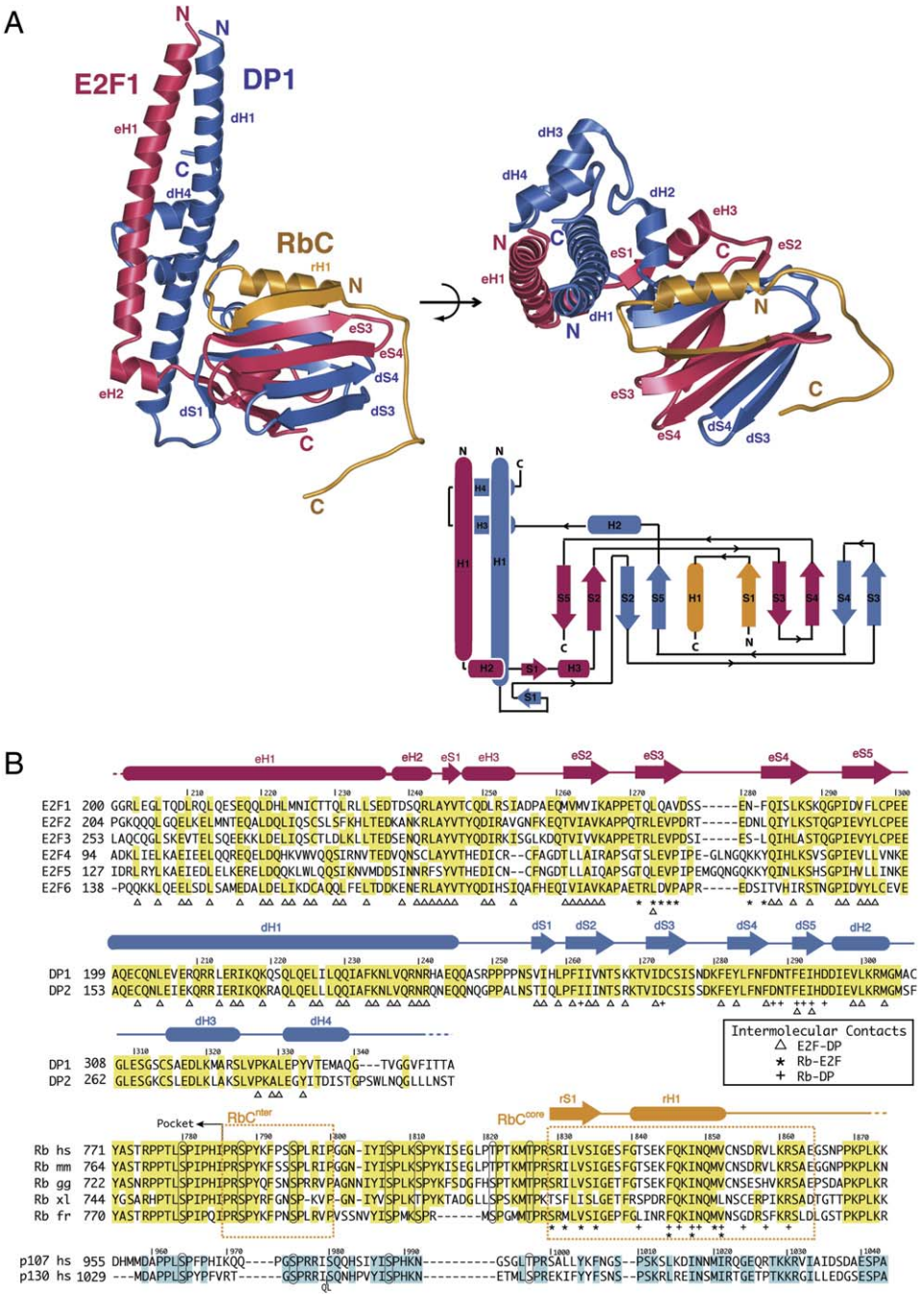

Figure 2. Overall structure and sequence alignment of the RbC^{core}-E2F1^{CM}-DP1^{CM} ternary complex

(A) E2F1^{CM} (red) and DP1^{CM} (blue) form an intertwined structure where both E2F1 and DP1 contact RbC^{core} (orange). Also shown is the E2F1^{CM}-DP1^{CM} topology diagram.

(B) Top panel shows sequence alignment of human E2F^{CM} and DP^{CM} family members. Lower panel shows sequence alignment of human (hs), mouse (mm), chicken (gg), frog (xl), and fugu (fr) RbC orthologs and of the human p107 and p130 Rb family members. Residues that are conserved among p107 and p130 orthologs are colored in cyan (see Supplemental Data, Section 4). Residues that make intermolecular contacts and the Rb/p107/p130 phosphorylation sites are marked. The positions of the RbC^{nter} and RbC^{core} motifs determined in this study are indicated by dotted boxes.

RbC^{core}-E2F1^{CM}-DP1^{CM} Interactions

The RbC fragment binds to the E2F1^{CM}-DP1^{CM} heterodimer using a strand-loop-helix motif (residues 829–852) and an extended segment (853–861). The RbC rS1 strand binds through six β sheet backbone hydrogen bonds (residues 831–835) to the E2F eS2 strand and through van der Waals

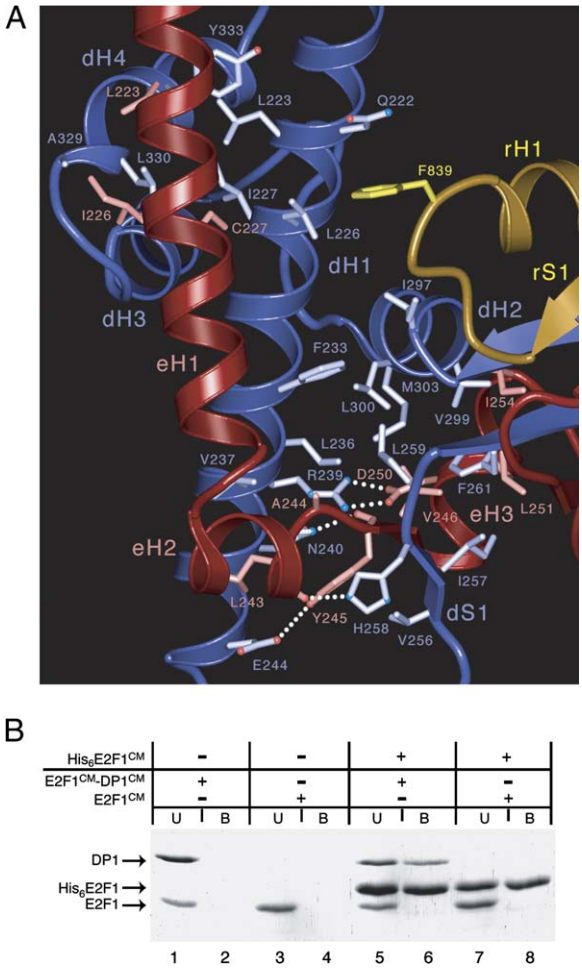

Figure 3. Structural and Biochemical Data Show E2Fs Prefer to Form Heterodimers with DP over Homodimers

(A) Close-up view of the interface between the coiled-coil and β sandwich domains that is formed by interactions between nonanalogous structural elements in E2F1 and DP1. These interactions, along with additional interactions in the coiled coil and the β sandwich (data not shown), indicate that an E2F homodimer would be less stable and structurally distinct from the heterodimer. Hydrogen bonds are marked by white dotted lines.

(B) Ten micromolar of purified His_6E2F1^{CM} was incubated overnight at 37ºC with 10 μM untagged $E2F1^{CM}$-$DP1^{CM}$ or $E2F1^{CM}$ alone and analyzed by Ni^{2+} precipitation as in Figure 1B.

contacts (Ile831, Val833, and Ile835) to hydrophobic residues from E2F1, DP1, and RbC rH1 (Figure 4A). The rH1 helix, which is amphipathic, makes multiple high-density van der Waals contacts (rH1 residues Phe845, Ile848, Met851, and Val852) to eS2 and dS4 residues in the exposed hydrophobic core of the β sandwich (Figure 4A). In addition, side chains from the polar face of rH1 make hydrogen bonds with backbone and side chain groups from DP1. For example, the side chain of Asn 849, invariant among Rb orthologs, makes bidentite hydrogen bonds with the backbone amide and carbonyl groups of Ile 293 of DP1 (Figure 4A). The intermolecular van der Waals and hydrogen bond contacts made by RbC are distributed approximately equally between E2F1 and DP1 atoms. The loop in between the rS1 strand and rH1 helix of RbC^{core} provides only a few minor intermolecular contacts (Figure 4A).

Following the rH1 helix, the RbC chain loops around the end of the β sandwich and a 7 residue extended segment makes additional hydrogen bonds with DP1 backbone and side chain groups (Figure 4A). After this extended segment, the last thirteen residues in the RbC construct used in crystallization (862–874) extend to and pack against another E2F1-DP1 complex related by a crystallographic 2-fold rotation symmetry. Deletion of these thirteen amino acids does not affect the affinity of RbC for the E2F1-DP1 complex (Figure 1B).

The structure of the RbC^{core}-$E2F1^{CM}$-$DP1^{CM}$ interface is in accord with our biochemical data showing that RbC binding is an activity common to both the E2F1 and E2F4 subfamilies. The E2F1 and DP1 residues that contact RbC^{core} are either conserved or conservatively substituted in E2F and DP paralogs (Figures 2B and 4A), and as discussed earlier, the interactions that form the E2F1-DP1 heterodimer involve residues conserved among E2F and DP paralogs (Figures 2B and 3A).

Inspection of the p107 C-terminal domain in light of the structure reveals that residues 999 to 1023 may represent a motif similar to RbC^{core}. This p107 sequence is evolutionarily conserved in p107 and p130 orthologs and is predicted to adopt a strand-loop-helix structure (Supplemental Data, Section 4). Most of the key E2F-DP interacting residues of RbC^{core}, such as Asn 849 that makes a pair of hydrogen bonds to DP1, are either conserved or conservatively substituted in this p107 segment (e.g., Asn 1018; Figure 2B). That residues 999 to 1023 of p107 are functionally analogous to RbC^{core} is supported by the observation that deletion of residues 1018–1068 compromises the ability of p107 to coimmunoprecipitate endogenous E2F from p107-transfected Saos2 cells (Zhu et al., 1995).

RbC^{core} Binding Requires E2F1-DP1 Heterodimerization

The structure indicates that the binding of RbC^{core} to E2F1 should strictly depend on the presence of DP1. To confirm this dependence, we incubated either 10 μM His_6-tagged $E2F1^{CM}$ or 10 μM heterodimeric His_6E2F1^{CM}-$DP1^{CM}$ with 100 μM $RbC^{814–874}$ and assayed for complex formation using the Ni^{2+} precipitation assay. Figure 4B shows that the resin containing His_6E2F1^{CM}-$DP1^{CM}$ had approximately a 1 molar ratio of $RbC^{814–874}$ eluted (Figure 4B, lane 4), whereas the resin containing His_6E2F1^{CM} alone had only trace amounts of $RbC^{814–874}$ eluted (Figure 4B, lane 6). In addition, we could not detect any ITC heat signal when $RbC^{814–874}$ was added to $E2F1^{CM}$ in the absence of $DP1^{CM}$ (Supplemental Data, Section 1). The dependence of RbC^{core} binding on DP1 observed here accounts for previous observations that heterodimerization of E2F with DP increases Rb and p107 binding in vitro and in vivo (Bandara et al., 1994; Beijersbergen et al., 1994; Helin et al., 1993b; Krek et al., 1993). Furthermore, the lack of DP in initial investigations of the Rb-E2F interaction may explain why the interaction described here was overlooked (Flemington et al., 1993; Helin et al., 1993a; Helin et al., 1992).

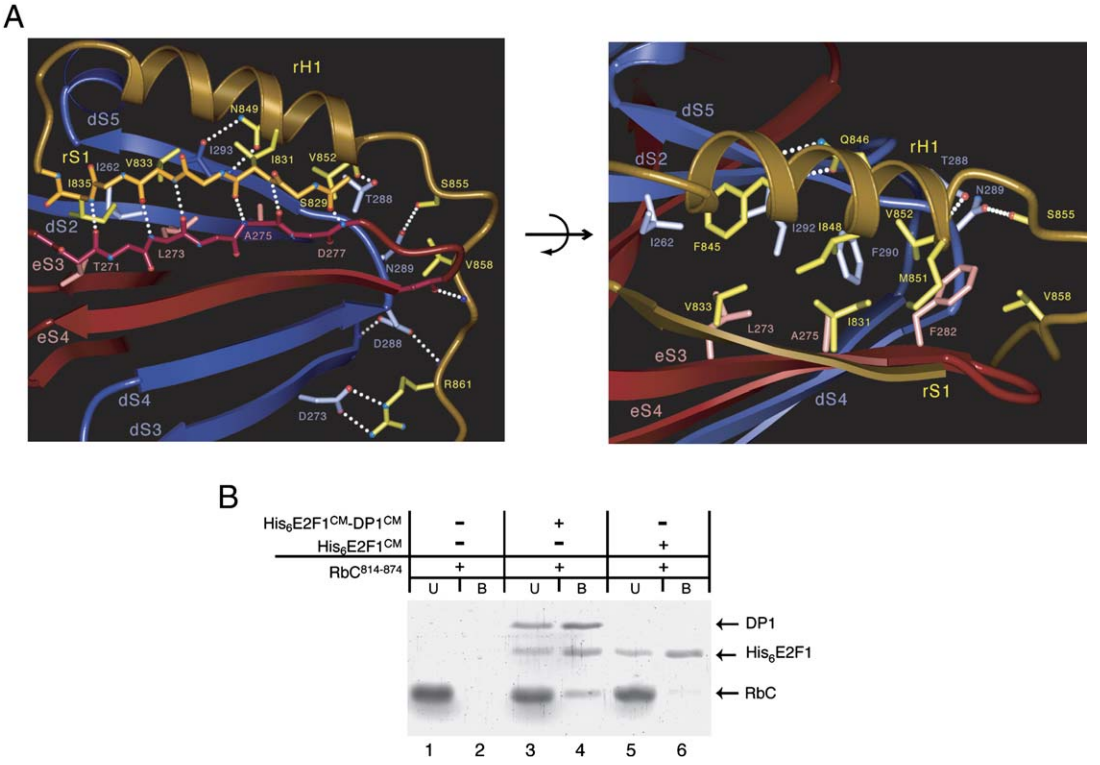

Figure 4. RbC^{core}-E2F1^{CM}-DP1^{CM} Interactions and the Requirement of DP1 for RbC^{core} Binding

(A) Close-up views of the interactions between RbC^{core} (orange) and E2F1^{CM}(red)-DP1^{CM} (blue) in two orthogonal orientations, showing that the interactions RbC^{core} makes are distributed approximately equally between E2F1 and DP1.

(B) Ten micromolar of purified His$_6$E2F1^{CM} or 10 μM of purified His$_6$E2F1^{CM}-DP1^{CM} were incubated with 100 μM RbC$^{814–874}$ and analyzed by Ni^{2+} precipitation as in Figure 1B.

The Secondary RbC^{nter}-E2F^{CM}-DP^{CM} Interaction Is Negatively Regulated by Phosphorylation of Ser 788/Ser 795

RbC contains six conserved Cdk-Cyclin sites, clustered in pairs, which are phosphorylated during G1 progression and the G1-S transition. Of these sites, the Ser 788/Ser 795 pair maps to the RbC^{nter} secondary E2F^{CM}-DP^{CM} interacting motif, and the Ser 807/Ser 811 and Thr 821/Thr 826 pairs map to the region between RbC^{nter} and RbC^{core} that our data show is uninvolved in E2F^{CM}-DP^{CM} binding. An additional site (Ser 780) is in the 771–785 segment at the end of the pocket domain that we included in our initial binding studies. These sites have been probed extensively by mutagenesis, but if and how they affect the phosphorylation-induced release of E2F has not been clear (Brown et al., 1999; Harbour et al., 1999; Knudsen and Wang, 1996; Knudsen and Wang, 1997). Our finding that the region encompassing Ser 788/Ser 795 makes up the RbC^{nter} secondary E2F^{CM}-DP^{CM} binding site raised the possibility that phosphorylation of Ser 788/Ser 795 affects the RbC^{nter}-E2F^{CM}-DP^{CM} interaction and contributes to the release of E2F-DP.

To investigate this possibility, we first asked if phosphorylation of RbC$^{771–928}$ affects its affinity for the E2F1^{CM}-DP1^{CM} complex. We phosphorylated RbC$^{771–928}$ using Cdk6 bound to a cyclin from the Kaposi's sarcoma-associated herpesvirus, shown to direct Cdk6/Cdk4 to phosphorylate both Cdk4/6-CyclinD- and Cdk2-CyclinA/E-specific sites (Godden-Kent et al., 1997). Use of this kinase resulted in the quantitative phosphorylation of all seven sites in RbC$^{771–928}$, as confirmed by reversed-phase HPLC and mass spectrometry (data not shown). ITC measurements with HPLC-purified, phosphorylated RbC$^{771–928}$ (phosRbC$^{771–928}$) showed that phosphorylation reduces the affinity of RbC$^{771–928}$ for the E2F1^{CM}-DP1^{CM} complex 22-fold, resulting in a K_d of 2.4 ± 0.2 μM that is comparable to the K_d of the RbC^{core} (Figure 5A). Phosphorylation of RbC$^{814–874}$, which consists of RbC^{core} and the preceding region with the Thr 821/Thr 826 phosphorylation sites, had little effect on its K_d for E2F^{CM}-DP^{CM} (phosRbC$^{814–874}$ K_d = 2.7 ± 1.1 μM, unphosphorylated RbC$^{814–874}$ K_d = 4.8 ± 0.9 μM; Figure 5A). Taken together, these data indicate that the secondary RbC^{nter}-E2F^{CM}-DP^{CM} interaction is essentially eliminated by the phosphorylation of Ser 788 and Ser 795, whereas the RbC^{core} interaction is not directly affected by the phosphorylation of any or all of the RbC sites.

Thr 821/Thr 826 Phosphorylation Induces Binding of RbC to the Pocket

Phosphorylation of RbC blocks the binding of viral proteins to the LxCxE binding site of the pocket, and mutation of Thr 821 and Thr 826 abolishes this effect (Knudsen and Wang, 1996). Based on these observations, it has been suggested

that an RbC segment containing the Thr 821/Thr 826 region may bind to the LxCxE binding site in the pocket intramolecularly (Harbour et al., 1999; Knudsen and Wang, 1996; Lee et al., 1998). If this interaction indeed occurs, then the proximity of Thr 821 and Thr 826 to the start of RbC^{core} interacting region (residue 829) raises the possibility that binding of the phosphorylated Thr 821/Thr 826 sequence to the pocket destabilizes the RbC^{core}-$E2F^{CM}$-DP^{CM} interactions.

To address this possibility, we first tested whether phosphorylation of $RbC^{814–874}$ induces binding to the Rb pocket using the Ni^{2+} precipitation assay. We incubated either 10 μM $His_6RbC^{814–874}$ or 10 μM $phosHis_6RbC^{814–874}$ with 10 μM Rb pocket (residues 372–787). Under these conditions, $phosHis_6RbC^{814–874}$ binds approximately 35% the Rb pocket input, whereas $His_6RbC^{814–874}$ binds only a trace amount (<2% of input, compare lanes 4 and 6 in Figure 5B). These data indicate that phosphorylation of Thr 821 and Thr 826 is sufficient to induce the binding of $RbC^{814–874}$ to the Rb pocket.

We next addressed whether phosphorylation of the nearby Ser 807 and Ser 811 sites, whose phosphorylation regulates the binding of the c-Abl kinase to Rb (Knudsen and Wang, 1996), can also induce binding to the Rb pocket. We incubated 10 μM Rb pocket with either 10 μM $His_6RbC^{801–874}$, which contains all four phosphorylation sites, or with 10 μM $RbC^{801–874}$(A821/A826), where Thr 821 and Thr 826 are mutated to alanines, and assayed binding using the Ni^{2+} precipitation assay. Figure 5C shows that whereas $phosRbC^{801–874}$ binds approximately 35% of the input Rb pocket, $phosRbC^{801–874}$(A821/A826) binds only trace amounts (compare lanes 4 and 6). These data demonstrate that specific phosphorylation at Thr 821 and Thr 826 is required for the binding of RbC to the pocket.

We next quantitated the binding of the Rb pocket to various RbC fragments using ITC. We found that whereas $phosRbC^{814–874}$ binds the Rb pocket with a K_d of 10 ± 1 μM, unphosphorylated $RbC^{814–874}$ gave no signal (Figure 5D). Consistent with results of the Ni^{2+} precipitation experiments, additional phosphorylation of Ser 807 and Ser 811 in a longer $phosRbC^{801–874}$ peptide or phosphorylation of all six sites in $phosRbC^{786–874}$ did not significantly affect the affinity (K_d = 8 ± 1 μM and K_d = 8 ± 4 μM, respectively; Figure 5C). These results indicate that phosphorylation of Thr 821 and Thr 826 is necessary and sufficient to induce the binding of $RbC^{814–874}$ to the Rb pocket and that phosphorylation of the other sites in $RbC^{786–874}$ does not affect this interaction.

The Rb pocket binds the E2F transactivation domain and the viral LxCxE motif at distinct sites (Lee et al., 2002; Lee et al., 1998; Xiao et al., 2003). To elucidate whether phosphorylated RbC binds the pocket at either of these sites, we tested if an HPV E7 LxCxE peptide, shown to bind the Rb pocket with a 0.11 μM K_d, or an E2F4 transactivation domain peptide could compete with the binding of phosphorylated RbC to the Rb pocket. Using the Ni^{2+} precipitation assay with all proteins at 10 μM, we found that the presence of 100 μM E2F4 transactivation-domain peptide does not affect the amount of Rb pocket that is bound by $His_6phosRbC^{814–874}$, but the presence of 100 μM LxCxE peptide results in only trace amounts of Rb pocket being bound by $His_6phosRbC^{814–874}$ (Figure 5E). This assay demonstrates that the binding sites for the phosphorylated RbC and for the viral LxCxE motif on the Rb pocket overlap substantially.

Binding of Phosphorylated RbC to the Pocket and to $E2F1^{CM}$-$DP1^{CM}$ Is Mutually Exclusive

Having established that phosphorylation of Thr 821/Thr 826 induces the binding of RbC to the Rb pocket, we next asked whether this interaction can interfere with the binding of RbC^{core} to the $E2F^{CM}$-DP^{CM} heterodimer. We preincubated increasing amounts (10 to 60 μM) of the Rb pocket with a constant amount (10 μM) of His_6E2F^{CM}-DP^{CM}, then added $phosRbC^{814–874}$ (10 μM) followed by Ni^{2+} precipitation and elution. In keeping with the ITC results, quantitation of the Coomassie-stained bands shows that in the absence of the Rb pocket His_6E2F1^{CM}-$DP1^{CM}$ binds 25% of the $phosRbC^{814–874}$ (Figure 5F, lane 2 and plot). The presence of 10 μM Rb pocket reduces the amount of $phosRbC^{814–874}$ coeluting with His_6E2F1^{CM}-$DP1^{CM}$ to 14% (Figure 5F, lane 4), and the presence of 30 and 60 μM Rb pocket reduces it further to 11% and 3%, respectively (Figure 5F, lanes 6 and 8). These results indicate that the binding of RbC to the Rb pocket and to $E2F1^{CM}$-$DP1^{CM}$ is mutually exclusive.

The simplest model that can account for this observation is that the Rb pocket and $E2F^{CM}$-DP^{CM} bind to partially overlapping regions of RbC, although other models involving steric or structural constraints are possible. To address this, we tested the binding of the Rb pocket either to $phosRbC^{818–839}$, which consists of the phosphorylated Thr 821/Thr 826 segment and the strand-loop region of RbC^{core}, and to $phosRbC^{818–828}$, which lacks any RbC^{core} residues. ITC measurements show that $phosRbC^{818–839}$ binds to the Rb pocket with a 7 ± 1 μM K_d, which is identical, within experimental error, to the K_d of the hyperphosphorylated entire RbC, whereas $phosRbC^{818–828}$ gave no ITC signal (Figure 5D). These data demonstrate that part of the $E2F1^{CM}$-$DP1^{CM}$ interacting region of RbC^{core} is also involved in binding to the Rb pocket, indicating that the binding of phosphorylated RbC to the pocket destabilizes the RbC^{core}-$E2F1^{CM}$-$DP1^{CM}$ interactions through direct competition. In the context of full-length Rb, the RbC-Rb pocket association will be intramolecular, which should allow the pocket to compete effectively with the RbC^{core}-$E2F1^{CM}$-$DP1^{CM}$ interactions and contribute to E2F release on phosphorylation. This conclusion is supported by a recent study showing that mutation of a patch of conserved lysine residues at the LxCxE binding site of the Rb pocket interferes with E2F-release by phosphorylation (Brown and Gallie, 2002).

DISCUSSION

Our structural and biochemical data establish that the C-terminal domains of the pocket proteins have a general E2F-DP binding activity. This activity resides in two segments, with a 36 residue RbC^{core} segment contributing the bulk of the binding energy with a K_d of 5 μM and a 15 residue RbC^{nter}

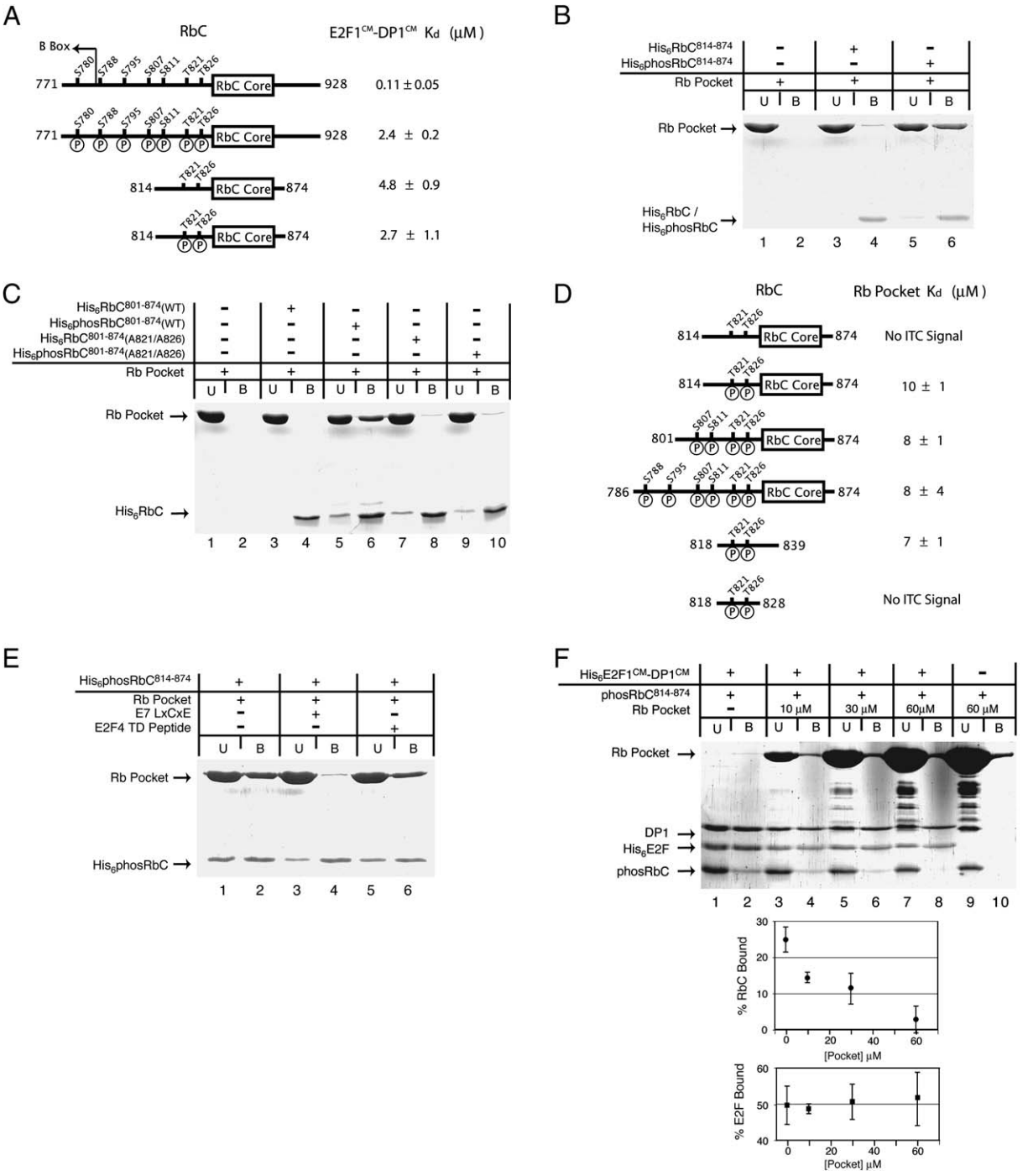

Figure 5. Phosphorylation of RbC Disrupts Binding to E2F1^{CM}-DP1^{CM}

(A) ITC measurements show that phosphorylation of all seven Cdk-Cyclin sites reduces the RbC-E2F1^{CM}-DP1^{CM} K_d 22-fold, essentially eliminating the RbC^{nter}-E2F1^{CM}-DP1^{CM} interactions, but does not affect the RbC^{core}-E2F1^{CM}-DP1^{CM} interactions.

(B) Phosphorylation of Thr 821/Thr 826 in RbC$^{814–874}$ (phosRbC$^{814–874}$) induces binding to the Rb pocket. Ten micromolar of purified His$_6$RbC$^{814–874}$ or His$_6$phosRbC$^{814–874}$ were incubated with 10 μM of purified Rb pocket and analyzed by Ni^{2+} precipitation assay as in Figure 1B.

(C) Binding of RbC to the Rb pocket is specific for phosphorylated Thr 821/Thr 826 (lane 6), and phosphorylated Ser 807/Ser 811 cannot substitute (lane 10). Ten micromolar of purified Rb pocket was incubated with either wild-type RbC$^{801–874}$ (His$_6$RbC$^{801–874}$[WT] or His$_6$phosRbC$^{801–874}$ [WT]) or the corresponding proteins where Thr 821 and Thr 826 were mutated to alanine (His$_6$RbC$^{801–874}$[A821/A826] and His$_6$phosRbC$^{801–874}$[A821/A826]). Reactions were analyzed as in (B).

(D) ITC-determined K_d values showing that RbC$^{818–839}$ consisting of the phosphorylated Thr 821/Thr 826 segment and the strand-loop region of RbC^{core} is necessary and sufficient to induce pocket binding.

segment increasing the affinity 36-fold, resulting in a K_d of 110 nM (Figures 1D and 6). This affinity is comparable to the 340–400 nM K_d values, determined by ITC, for the association of the Rb pocket domain with the E2F1 transactivation domain (Lee et al., 1998; Xiao et al., 2003), indicating that the RbC-E2F1^{CM}-DP1^{CM} interactions are likely to be as important as the Rb pocket-E2F transactivation domain interactions for Rb-E2F-DP assembly.

Our biochemical data show that RbC can bind to the CC-MB domains of E2F1-DP1, E2F2-DP2, E2F4-DP2, and E2F1-DP5 comparably (Figure 1B), and our ITC data demonstrate that the RbC-E2F1^{CM}-DP1^{CM} and RbC-E2F4^{CM}-DP2^{CM} complexes have essentially identical K_d values (Figure 1C). Together with the conservation of the Rb-E2F-DP contacts in the crystal structure, our findings indicate that the RbC-E2F^{CM}-DP^{CM} interaction is general across members of both E2F-DP subfamilies. This common interaction mirrors the similar affinities of the Rb pocket domain for the transactivation domains of the two E2F subfamilies (Lee et al., 2002; Lee et al., 1998; Xiao et al., 2003). Our data also show that the C-terminal domain of p107 binds to E2F4^{CM}-DP1^{CM} with high affinity but binds to E2F1^{CM}-DP1^{CM} ~6-fold weaker (Figure 1C). This result indicates that the preferential association of p107 with E2F4 is due, at least in part, to the C-terminal E2F-DP binding activity of p107.

The general E2F-DP binding activity demonstrated here explains the well-established but poorly understood requirement for the C-terminal domains of the pocket proteins for high-affinity E2F-DP binding (Hiebert, 1993; Hiebert et al., 1992; Qin et al., 1992). It also can account, at least in part, for the findings that the C-terminal domains of the pocket proteins are absolutely required for full repression of E2F-responsive promoters and for growth suppression (Qin et al., 1992; Zhu et al., 1995). Finally, considering recent work identifying interactions between E2F MB domains and other transcription factors that result in gene-specific activation (Giangrande et al., 2004; Schlisio et al., 2002), it is possible that the RbC-MB interaction described here provides an additional mechanism by which Rb can control E2F transcriptional output.

The RbC-E2F^{CM}-DP^{CM} interaction critically depends on E2F-DP heterodimerization. Our structural data show that the contacts RbC makes to E2F1 and DP1 are comparable in number and suggest that the E2F1^{CM}-DP1^{CM} structure would not form by E2F1^{CM} alone (Figures 3 and 4). In support, our biochemical data show that E2F1^{CM} does not bind RbC detectably (Figure 4B), and E2F1^{CM} alone does not homodimerize stably (Figure 3B; Supplemental Data, Section 2). The requirement for DP thus explains why many past studies, which typically were carried out with E2F alone, failed to find evidence for a direct interaction between RbC and E2F.

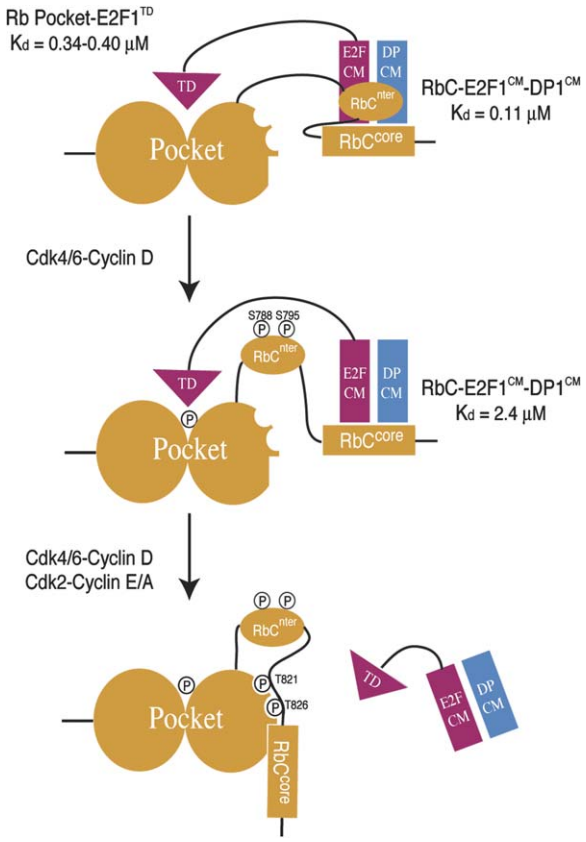

Figure 6. Model for the Phosphorylation-Induced Dissociation of the RbC-E2F^{CM}-DP^{CM} Interfaces, Incorporating Reported Data on the Rb Pocket-E2F TD Association

Unphosphorylated Rb binds E2F-DP heterodimers through at least three interactions. The Rb pocket binds to the E2F TD, and RbC^{nter} and RbC^{core} bind to the E2F^{CM}-DP^{CM} domains. In early G1, phosphorylation of Ser 788/Ser 795 by Cdk4-CyclinD induces dissociation of RbC^{nter} reducing the overall RbC-E2F^{CM}-DP^{CM} affinity. Subsequent phosphorylation of Thr 821/Thr 826 induces an intramolecular interaction between RbC and the Rb pocket that excludes the binding of RbC^{core} to E2F^{CM}-DP^{CM} Phosphorylation of other sites in the pocket likely disrupts the binding of the E2F transactivation domain.

A general interaction between the C-terminal domains of the pocket proteins and E2F-DP heterodimers was anticipated by studies of the mechanism through which viral proteins displace E2F (Jost et al., 1996; O'Connor and Hearing, 1994; Patrick et al., 1994; Raychaudhuri et al., 1991; Zalvide et al., 1998). However, the only previous direct experimental

(E) Binding of phosRbC$^{814–874}$ to the Rb pocket is competed by the HPV E7 LxCxE peptide but not by the E2F4 TD peptide. The same assay was performed as in (B), except for the addition of a 10-fold molar excess of either an HPV E7 LxCxE peptide or an E2F4 TD peptide.

(F) Binding of phosRbC$^{814–874}$ to the Rb pocket excludes binding of phosRbC$^{814–874}$ to E2F^{CM}-DP^{CM}. Ten micromolar of His$_6$E2F1^{CM}-DP1^{CM} was mixed with phosRbC$^{814–874}$ in the absence or presence of increasing concentrations of Rb pocket. Percent RbC bound, calculated from the integrated intensity of Coomassie-stained bands as (RbC bound)/(RbC bound + RbC unbound) for each pair of lanes, decreases with increasing Rb pocket concentration. Percent His$_6$E2F1^{CM} bound, calculated analogously, remains constant. Data from two separate experiments were averaged, and the error bars correspond to the standard deviations of the two measurements. A small amount of Rb pocket was observed in the bound fractions independent of His$_6$E2F1^{CM}-DP1^{CM} (lane 10). We presume that it is a result of nonspecific interactions between the Rb pocket and the Ni^{2+} resin.

evidence for this idea has been a recent study by Dick and Dyson (2003), in which an interaction between an Rb C-terminal fragment and E2F1-DP1 was shown to be specific for E2F1 and responsible for the unique ability of E2F1 to induce apoptosis. Their conclusions were based in part on the findings that a GST-tagged $Rb^{792–928}$ fragment, which lacks part of the RbC^{nter} motif identified here, binds to HA-tagged E2F1-DP1 as well as HA-E2F1(1–374)-DP1 lacking the transactivation domain, but it does not bind HA-E2F4-DP1 and binds HA-E2F2-DP1 100-fold weaker than HA-E2F1-DP1 in an indirect assay. It is not clear why these findings differ from our results demonstrating that the RbC-$E2F^{CM}$-DP^{CM} interaction is common to both E2F subfamilies. The use of mammalian cell-expressed proteins and the presence of cell extracts in the binding assays of Dick and Dyson (2003) might have resulted in differentially phosphorylated proteins and contributed to the differences. Differences in the protein fragment boundaries used in the two studies might also have been a contributing factor. In this respect, it is possible that the interaction described by Dick and Dyson (2003) is only partially overlapping with or is distinct from the one demonstrated here (Supplemental Data, Section 5).

The RbC-$E2F^{CM}$-DP^{CM} interaction described here also provides a basis for the first mechanistic description of how the Rb-E2F-DP complex is dissociated by phosphorylation, a key event in the control of the G1-S transition (Figure 6). We show that phosphorylation of Ser 788/Ser 795 in RbC^{nter} essentially eliminates the secondary interaction in the RbC-$E2F^{CM}$-DP^{CM} complex, weakening its K_d 22-fold (Figures 5A and 6). Phosphorylation of Ser 795, which is an efficient Cdk4/6-CyclinD phosphorylation site occurs early in G1 (Connel-Crowley et al., 1997; Lundberg and Weinberg, 1998; Pan et al., 1998), suggesting that the elimination of the RbC^{nter}-$E2F^{CM}$-DP^{CM} interaction is an early event in the destabilization of the Rb-E2F-DP complex by phosphorylation. Our data show that the remaining RbC^{core}-$E2F^{CM}$-DP^{CM} interactions are eliminated indirectly by the subsequent phosphorylation of the Thr 821/Thr 826 Cdk2-CyclinE/A sites. This phosphorylation induces the binding of pThr 821/pThr 826 and part of the following RbC^{core} strand-loop segment to the Rb pocket in a manner that directly competes with binding of RbC^{core} to $E2F^{CM}$-DP^{CM} (Figure 6).

The phosphorylation-mediated dissociation of RbC from $E2F^{CM}$-DP^{CM} should destabilize the overall Rb-E2F-DP complex significantly, consistent with the Rb pocket-E2F transactivation domain interaction not being sufficient for full transcriptional repression and for growth suppression (Hiebert, 1993; Hiebert et al., 1992; Qin et al., 1992). However, the Rb pocket-E2F transactivation domain interactions are also likely regulated by phosphorylation. Phosphorylation of Ser 608/Ser 612 in the Rb pocket inhibits the binding of E2F1 in a manner that is dependent on the presence of the Rb N-terminal domain (Knudsen and Wang, 1997). This observation suggests that a phosphorylation-induced intramolecular interaction between the Rb pocket and N-terminal domains, reminiscent of the pocket-RbC interaction demonstrated here, may negatively regulate E2F transactivation domain binding.

Our findings also establish that at least one reason for the existence of the LxCxE binding site is intramolecular interactions. The crystal structure of the Rb pocket domain bound to the HPV E7 LxCxE motif showed that the LxCxE binding site is one of the features best conserved in Rb orthologs and the p107/p130 paralogs (Lee et al., 1998). Although several cellular proteins have been reported to bind Rb through LxCxE-like sequences, none have been demonstrated to bind to the LxCxE site directly and with an affinity commensurate with the conservation of this site. In fact, a recent study showed that mutations in the Rb pocket that prevent the binding of LxCxE peptides do not affect the ability of Rb to bind to HDAC1, repress E2F-responsive promoters and arrest the cell cycle (Dick et al., 2000). The pThr 821/pThr 826-strand-loop RbC segment that our data show binds to the LxCxE binding site is highly conserved in Rb orthologs and a similar motif appears to be present in p107 as well (Figure 2B). This intramolecular interaction may well account, at least in part, for the presence and conservation of the LxCxE binding site in the pocket proteins.

EXPERIMENTAL PROCEDURES

Protein Expression, Purification, and Phosphorylation

Recombinant human $E2F^{CM}$ and DP^{CM} proteins (E2F1 residues 200–301, E2F2 residues 206–306, E2F4 residues 91–198, E2F5 residues 125–232, DP1 residues 199–350, and DP2 residues 153–307) were coexpressed as His_6 and glutathione S-transferase (GST) fusion proteins, respectively, in *Escherichia coli*. Coexpression was achieved as reported previously either by transforming with one plasmid containing a dicistronic message or with two plasmids containing distinct origins of replication (p15A and pBR322; Stebbins et al., 1999). The $E2F^{CM}$-DP^{CM} complexes were purified first with Ni^{2+}-NTA then with glutathione Sepharose affinity chromatography, and following cleavage of the tags where indicated, by anion-exchange chromatography. His_6-tagged human RbC, p107C, and E2F1 transactivation-domain (372–437) polypeptides were expressed in *E. coli*. They were first purified by Ni^{2+} affinity chromatography in the presence of 6 M urea, then by ion-exchange chromatography in the absence of urea. Where indicated, His_6-tag cleavage was followed by repurification with ion-exchange chromatography. The human Rb pocket domain (residues 372–787) was purified as described previously, except the linker between the two domains was intact (Lee et al., 1998). RbC polypeptides were phosphorylated with an ~100 nM Cdk6-herpesvirus cyclin kinase preparation (Jeffrey et al., 2000), at 37ºC in a buffer of 50 mM Tris-HCl, 10 mM $MgCl_2$, 0.1 mM Na_3VO_4 (pH 7.0), with 1mM ATP per phosphorylation site and ~0.1 mM polypeptide. Phosphorylation was nearly quantitative, as determined by reverse-phase HPLC and mass spectrometry. Following phosphorylation, the polypeptides were repurified by reversed-phase HPLC. The HPV E7 LxCxE (residues 19–31), E2F4 transactivation domain (390–407), $RbC^{818–839}$, and $RbC^{818–828}$ peptides were synthesized, N-terminal acetylated, and C-terminal amidated and purified by reversed-phase HPLC. Protein and peptide concentrations were determined from A_{280} measurements using calculated extinction coefficients.

Crystallization

Purified RbC (residues 829–874) was mixed with purified $E2F1^{CM}$-$DP1^{CM}$ complex at a 2:1 molar ratio, and the ternary complex was isolated using Superdex75 gel-filtration chromatography and concentrated to 20 mg/ml^{-1} in a buffer of 25 mM Tris-HCl, 200 mM NaCl, and 5 mM DTT (pH 8.0). Crystals were grown by the hanging-drop vapor diffusion method at room temperature from 100 mM sodium citrate, 1.6 M ammonium sulfate, and 8% w/v PEG 400 (pH 5.5). Details of X-ray diffraction data collection and analysis are reported in Supplemental Data, Section 6.

Ni^{2+}-His_6 Affinity Precipitation Assays

Indicated proteins were incubated at room temperature for 5 min in 40 μl of binding buffer consisting of 50 mM Tris-HCl, 75 mM NaCl, and 15 mM imidazole (pH 7.1) prior to addition of 15μl Ni^{2+}-NTA resin. After 5 min, the resin was spun down, and the ~40 μl supernatant, marked as the unbound (U) fraction in the figures, was removed. The resin was then washed twice with 1 ml of binding buffer and the Ni^{2+} bound proteins were eluted with 40 μl of binding buffer supplemented with 600 mM imidazole. One-fourth of each of the supernatant and eluted fractions, marked as the unbound (U) and bound (B) fractions, respectively, on the figures, were fractionated by SDS-PAGE and were stained with Coomassie. The protein concentrations used in the incubations were all 10 μM, except when indicated otherwise. For Figure 3B, proteins were incubated overnight at 37ºC to allow for dimer exchange. The Rb pocket competition titration (Figure 5F) was quantified using ImageGauge software.

Isothermal-Titration Calorimetry

Isothermal calorimetry experiments were performed with a Micro Calorimetry System (Microcal Inc.). Typically, 0.3–1 mM RbC, phosRbC, or p107 polypeptides were injected into a 20–50 μM solution of $E2F^{CM}$-DP^{CM} or Rb pocket. Experiments were done at 25ºC in 50 mM Tris-HCl, 100 mM NaCl, and 2 mM DTT (pH 7.0). Titration data were analyzed using the MicroCal Origin software, and the reported binding constants and standard deviations were derived from two to four independent measurements. Sample titration data are shown in Supplemental Data, Section 1.

Supplemental Data

Supplemental Data include three figures and supplemental text and can be found with this article online at http://www.cell.com/cgi/content/full/123/6/1093/DC1/.

ACKNOWLEDGMENTS

We thank Dr. David King of the HHMI mass spectrometry laboratory for analysis, Dr. A.T. Phan for assistance with NMR spectroscopy data collection, the staff of the National Synchrotron Light Source X4A and Advanced Photon Source ID-24 beamlines for help with X-ray diffraction data collection, and N. Thoma, B. Hao, and P.D. Jeffery for useful discussions. This work was supported by the NIH, the Howard Hughes Medical Institute, and the Dewitt Wallace Foundation. S.M.R. is a Damon Runyon Fellow supported by the Damon Runyon Cancer Research Foundation.

Received: August 8, 2005
Revised: September 14, 2005
Accepted: September 21, 2005
Published: December 15, 2005

REFERENCES

Adams, P.D., Li, X., Sellers, W.R., Baker, K.B., Leng, X., Harper, J.W., Taya, Y., and Kaelin, W.G.J. (1999). Retinoblastoma protein contains a C-terminal motif that targets it for phosphorylation by cyclin-cdk complexes. Mol. Cell. Biol. *19*, 1068–1080.

Bandara, L.R., Buck, V.M., Zamanian, M., Johnston, L.H., and La Thangue, N.B. (1993). Functional synergy between DP-1 and E2F-1 in the cell cycle-regulating transcription factor DRTF1/E2F. EMBO J. *12*, 4317–4324.

Bandara, L.R., Lam, E.W.-F., Sorensen, T.S., Zamanian, M., Girling, R., and La Thangue, N.B. (1994). DP-1: a cell cycle-regulated and phosphorylated component of transcription factor DRTF1/E2F which is functionally important for recognition by pRb and the adenovirus E4 orf 6/7 protein. EMBO J. *13*, 3104–3114.

Beijersbergen, R.L., Kerkhoven, R.M., Zhu, L., Carlee, L., Voorhoeve, P.M., and Bernards, R. (1994). E2F-4, a new member of the E2F gene family, has oncogenic activity and associates with p107 in vivo. Genes Dev. *8*, 2680–2690.

Bork, P., Holm, L., and Sander, C. (1994). The immunoglobulin fold: structural classification, sequence patterns and common core. J. Mol. Biol. *242*, 309–320.

Brown, V.D., and Gallie, B.L. (2002). The B-domain lysine patch of pRB is required for binding to large T antigen and release of E2F by phosphorylation. Mol. Cell. Biol. *22*, 1390–1401.

Brown, V.D., Phillips, R.A., and Gallie, B.L. (1999). Cumulative effect of phosphorylation of pRb on regulation of E2F activity. Mol. Cell. Biol. *19*, 3246–3256.

Chellappan, S.P., Hiebert, S.W., Mudryj, M., Horowitz, J.M., and Nevins, J.R. (1991). The E2F transcription factor is a cellular target for the Rb protein. Cell *65*, 1053–1061.

Connel-Crowley, L., Harper, J.W., and Goodrich, D.W. (1997). Cyclin D1/Cdk4 regulates retinoblastoma protein-mediated cell cycle arrest by site-specific phosphorylation. Mol. Biol. Cell *8*, 287–301.

Dick, F.A., and Dyson, N. (2003). pRB contains an E2F1-specific binding domain that allows E2F1-induced apoptosis to be regulated separately from other E2F activities. Mol. Cell *12*, 639–649.

Dick, F.A., Sailhamer, E., and Dyson, N. (2000). Mutagenesis of the pRB pocket reveals that cell cycle arrest functions are separable from binding to viral oncoproteins. Mol. Cell. Biol. *20*, 3715–3727.

Dyson, N. (1998). The regulation of E2F by pRB-family proteins. Genes Dev. *12*, 2245–2262.

Flemington, E.K., Speck, S.H., and Kaelin, W.G.J. (1993). E2F-1-mediated transactivation is inhibited by complex formation with the retinoblastoma susceptibility gene product. Proc. Natl. Acad. Sci. USA *90*, 6914–6918.

Giangrande, P.H., Zhu, W., Rempel, R.E., Laakso, N., and Nevins, J.R. (2004). Combinatorial gene control involving E2F and E box family members. EMBO J. *23*, 1336–1347.

Godden-Kent, D., Talbot, S.J., Boshoff, C., Chang, Y., Moore, P., Weiss, R.A., and Mittnacht, S. (1997). The cyclin encoded by Kaposi's sarcoma-associated herpesvirus stimulates cdk6 to phosphorylate the retinoblastoma protein and histone H1. J. Virol. *71*, 4193–4198.

Harbour, J.W., Luo, R.X., DeiSanti, A., Postigo, A.A., and Dean, D.C. (1999). Cdk phosphorylation triggers sequential intramolecular interactions that progressively block Rb functions as cells move through G1. Cell *98*, 859–869.

Helin, K., Lees, J.A., Vidal, M., Dyson, N., Harlow, E., and Fattaey, A. (1992). A cDNA encoding a pRB-binding protein with properties of the transcriptional factor E2F. Cell *70*, 337–350.

Helin, K., Harlow, E., and Fattaey, A. (1993a). Inhibition of E2F-1 transactivation by direct binding of the retinoblastoma protein. Mol. Cell. Biol. *13*, 6501–6508.

Helin, K., Wu, C.-L., Fattaey, A.R., Lees, J.A., Dynlacht, B.D., Ngwu, C., and Harlow, E. (1993b). Heterodimerization of the transcription factors E2F-1 and DP-1 leads to cooperative trans-activation. Genes Dev. *7*, 1850–1861.

Hiebert, S.W. (1993). Regions of the retinoblastoma gene product required for its interaction with the E2F transcription factor are necessary for E2 promoter repression and pRb-mediated growth suppression. Mol. Cell. Biol. *13*, 3384–3391.

Hiebert, S.W., Chellappan, S.P., Horowitz, J.M., and Nevins, J.R. (1992). The interaction of RB with E2F coincides with an inhibition of the transcriptional activity of E2F. Genes Dev. *6*, 177–185.

Huber, H.E., Edwards, G., Goodhart, P.J., Patrick, D.R., Huang, P.S., Ivey-Hoyle, M., Barnett, S.F., Oliff, A., and Heimbrook, D.C. (1993). Transcription factor E2F binds DNA as a heterodimer. Proc. Natl. Acad. Sci. USA *90*, 3525–3529.

Jeffrey, P., Tong, L., and Pavletich, N.P. (2000). Structural basis of inhibition of CDK-cyclin complexes by INK4 inhibitors. Genes Dev. *14*, 3115–3125.

Jost, C., Ginsberg, D., and Kaelin, W.G.J. (1996). A conserved region of unknown function participates in the recognition of E2F family members by the adenovirus E4 ORF 6/7 protein. J. Virol. *220*, 78–90.

Knudsen, E.S., and Wang, J.Y.J. (1996). Differential regulation of retinoblastoma function by specific cdk phosphorylation sites. J. Biochem. (Tokyo) *271*, 8313–8320.

Knudsen, E.S., and Wang, J.Y.J. (1997). Dual mechanisms for the inhibition of E2F binding to RB by cyclin-dependent kinase-meditated RB phosphorylation. Mol. Cell. Biol. *17*, 5771–5783.

Krek, W., Livingston, D.M., and Shirodkar, S. (1993). Binding to DNA and the retinoblastoma gene product promoted by complex formation of different E2F family members. Science *262*, 1557–1560.

Lee, J.-O., Russo, A.A., and Pavletich, N.P. (1998). Structure of the retinoblastoma tumour-suppressor pocket domain bound to a peptide from HPV E7. Nature *391*, 859–865.

Lee, C., Chang, J.H., Lee, H.S., and Cho, Y. (2002). Structural basis for the recognition of the E2F transactivation domain by the retinoblastoma tumor suppressor. Genes Dev. *16*, 3199–3212.

Lundberg, A.S., and Weinberg, R.A. (1998). Functional inactivation of the retinoblastoma protein requires sequential modification by at least two distinct cyclin-cdk complexes. Mol. Cell. Biol. *18*, 753–761.

Lupas, A. (1996). Coiled coils: new structures and new functions. Trends Biochem. Sci. *21*, 375–382.

Nevins, J.R. (1994). Cell cycle targets of the DNA tumor viruses. Curr. Opin. Genet. Dev. *4*, 130–134.

O'Connor, R.J., and Hearing, P. (1994). Mutually exclusive interaction of the adenovirus E4-6/7 protein and the retinoblastoma gene product with internal domains of E2F-1 and DP-1. J. Virol. *68*, 6848–6862.

Pan, W., Sun, T., Hoess, R.H., and Grafstrom, R.H. (1998). Defining the minimal portion of the retinoblastoma protein that serves as an efficient substrate for cdk4 kinase/cyclin D1 complex. Carcinogenesis *19*, 765–769.

Pan, W., Cox, S., Hoess, R.H., and Grafstrom, R.H. (2001). A cyclin D1/cyclin-dependent kinase 4 binding site within the C domain of the retinoblastoma protein. Cancer Res. *61*, 2885–2891.

Patrick, D.R., Oliff, A., and Heimbrook, D.C. (1994). Identification of a novel retinoblastoma gene product binding site on the human papillomavirus type 16 E7 protein. J. Biochem. (Tokyo) *269*, 6842–6850.

Qin, X., Chittenden, T., Livingston, D.M., and Kaelin, W.G.J. (1992). Identification of a growth suppression domain within the retinoblastoma gene product. Genes Dev. *6*, 953–964.

Raychaudhuri, P., Bagchi, S., Devoto, S.H., Kraus, V.B., Moran, E., and Nevins, J.R. (1991). Domains of the adenovirus E1A protein required for oncogenic activity are also required for dissociation of E2F transcription factor complexes. Genes Dev. *5*, 1200–1211.

Schlisio, S., Halperin, T., Vidal, M., and Nevins, J.R. (2002). Interaction of YY1 with E2Fs, mediated by RYBP, provides a mechanism for specificity of E2F function. EMBO J. *21*, 5775–5786.

Sherr, C.J. (1996). Cancer cell cycles. Science *274*, 1672–1677.

Stebbins, C.E., Kaelin, W.G.J., and Pavletich, N.P. (1999). Structure of the VHL-ElonginC-ElonginB complex: implications for VHL tumor suppressor function. Science *284*, 455–461.

Trimarchi, J.M., and Lees, J.A. (2002). Sibling rivalry in the E2F family. Nat. Rev. Mol. Cell Biol. *3*, 11–19.

Wallace, M., and Ball, K. (2004). Docking-dependent regulation of the Rb tumor suppressor protein by Cdk4. Mol. Cell. Biol. *24*, 5606–5619.

Weinberg, R.A. (1995). The retinoblastoma protein and cell cycle control. Cell *81*, 323–330.

Xiao, B., Spencer, J., Clements, A., Ali-Khan, N., Mittnacht, S., Broceno, C., Burghammer, M., Perrakis, A., Marmorstein, R., and Gamblin, S.J. (2003). Crystal structure of the retinoblastoma tumor suppressor protein bound to E2F and the molecular basis of its regulation. Proc. Natl. Acad. Sci. USA *100*, 2363–2368.

Zalvide, J., Stubdal, H., and DeCaprio, J.A. (1998). The J domain of Simian Virus 40 large T antigen is required to functionally inactivate Rb family proteins. Mol. Cell. Biol. *18*, 1408–1415.

Zheng, N., Fraenkel, E., Pabo, C.O., and Pavletich, N.P. (1999). Structural basis of DNA recognition by the heterodimeric cell cycle transcription factor E2F-DP. Genes Dev. *13*, 666–674.

Zhu, L., Enders, G., Lees, J.A., Beijersbergen, R.L., Bernards, R., and Harlow, E. (1995). The pRb-related protein p107 contains two growth suppression domains: independent interactions with E2F and cyclin/cdk complexes. EMBO J. *14*, 1904–1913.

Accession Numbers

The coordinates for the structure described in this work have been deposited in the Protein Data Bank under ID code 2AZE.